Liquid Jet Instability and Dynamic Surface Tension Effect on Breakup

Lisong Yang and Colin D Bain; Chemistry Department, Durham University, DH 1 3LE, UK

Abstract

We studied the instability of a liquid jet by confocal microscopy, a non-invasive three-dimensional imaging technique. The amplitude of jet oscillation can be measured from its early stage to the vicinity of the jet breakup with a radial resolution of 80 nm. A continuous jet with a diameter of 100 μm and mean velocity of 5.6 ms^{-1} was perturbed at a frequency of 11.8 kHz. The growth rate of the sinusoidal instability was used to determine the dynamic surface tension of water and of surfactant solutions at a surface age of ≤ 1 ms, using an established linear, axisymmetric, constant property model. A commercial aqueous non-ionic Gemini surfactant Surfynol 465 reduced the dynamic surface tension more efficiently than an anionic surfactant sodium dodecyl sulphate (SDS). The effect of surfactant on the jet breakup length has also been studied. We applied the confocal imaging system to study the temporal evolution of a ligament which starts from a concave neck and eventually develops into a satellite drop. The pinch-off process has been studied in detail. It is found that the final stages of ligament rupture are the same for water and surfactant solutions. The time taken for the satellite drop to be engulfed by the following drop depends on the surfactant concentration.

Introduction

Surfactants (a contraction of surface active agents) can reduce the surface tension of liquids even at low bulk concentrations. They are widely used in many industrial, agricultural and biological processes. For example, surfactants are commonly added to inkjet inks as wetting, emulsifying and dispersing agents. By lowering the surface tension of inks, surfactants can improve the wettability or printability of the inks. The reduction of the surface tension by surfactant is a dynamic process where molecules must first diffuse to the surface from the bulk and then orient themselves at the interface. Many experimental techniques have been developed over the past decades to measure dynamic surface tension (DST) and study the adsorption mechanism, including the maximum-bubble-pressure, oscillating-jet, overflowing-cylinder and drop shape analysis methods [1]. However these techniques can only provide us DST with surface age older than 1 ms. In fact, efficient surfactants can lower the surface tension to its equilibrium value within 1 ms at concentrations of <1%. Take an anionic surfactant sodium dodecyl sulphate (SDS) as an example. It has a critical micelle concentration (cmc) of 8 mM in water, i.e. 0.23% by wt, and the equilibrium value of the surface excess at this concentration is $\Gamma_{cmc} \approx 4 \times 10^{-6}$ mol m^{-2}. Given that SDS adsorption is diffusion controlled, the diffusion time τ_d is defined as the mean time taken by a surfactant molecule to diffuse a distance given by the depletion length Γ/c, where c is the bulk surfactant concentration. [2]:

$$\tau_d = \frac{1}{2D}\left(\frac{\Gamma}{c}\right)^2 . \quad (1)$$

The diffusion coefficient of SDS is ~ 5×10^{-10} m^2 s^{-1} which gives τ_d ~ 0.25 ms at its cmc. The time taken for a freshly formed surface to reach equilibrium is ~ $5\tau_d \approx$ 1 ms. Hence to measure the DST in sub-millisecond or shorter timescale will be of great interest for scientific research and industrial application.

In this paper, we present our experimental study on the instability of a continuous liquid jet. The growth rate of the liquid jet in the presence of two types of surfactants has been measured by confocal imaging. The DST of the liquid at a surface age of ≤ 1 ms can be determined via growth rate measurement. The surfactant effect on the jet breakup and satellite drop formation has also been studied in detail.

Experiments

The experimental apparatus is shown in Figure 1: the details will be presented elsewhere [3]. The pressurised liquid is guided from a reservoir into a dispenser head. A pressure control unit and a liquid pump are adjusted to keep the reservoir liquid volume constant so as to guarantee a constant liquid flow rate. A laminar jet emerges from the dispenser head through a funnel-shaped glass nozzle with an exit diameter of 100 μm into free air at a room temperature of 22 °C. The jet is mounted in a three-dimensional motorised translation stage with an actuator travel range of 12.5 mm and an accuracy of 0.2 μm. A TTL signal generator is applied to the valve control. The flow rate for the partially closed micro-valve inside the disperser head is about 98% of that for an open valve. The amplitude of the applied periodic perturbation on the jet is therefore small.

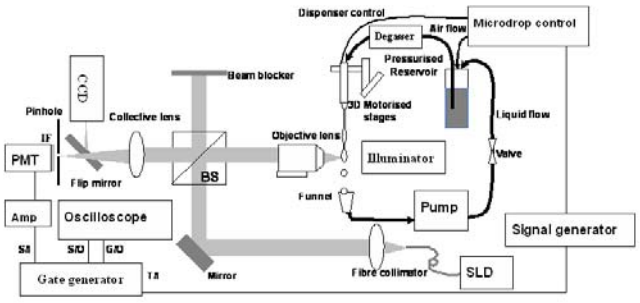

***Figure 1**. Experimental setup. SLD: superluminescent diode; BS: beamsplitter; PMT: photomultiplier tube; Amp: amplifier. S/I: signal-in; S/O: signal-out; T/I: trigger-in; G/O: gate-out.*

We used UHQ water from Millipore water purification system (Millipore Corporation, USA) as a calibration fluid in the jet, assuming it to have a constant surface tension. Two types of surfactants were chosen. A simple single-chain anionic surfactant

(SDS, Sigma-Aldrich, 99+%) with molecular weight M_w of 288.38 g mol^{-1} was recrystallized three times from 99.9% Ethanol (Fisher). A nonionic gemini surfactant Surfynol 465 (ethoxylated 2,4,7,9-tetramethyl-5-decyne-4,7-diol containing 10 mol of ethylene oxide per molecule, Air Products), comprises two hydrophilic heads connected by a molecular segment and two hydro-phobic tails with M_w of 666 g mol^{-1}. Surfynol 465 has a hydrophilic-lipophilic balance value of 13 which makes it water soluble up to concentrations greater than 1.0%. In order to minimize the formation of bubbles in the surfactant solution, which may cause uneven wetting of the nozzle plate and drop misdirection, an inline degasser and vacuum pump are used in the input line of the dispenser. Aqueous Surfynol 465 foams much less than SDS.

For visualization, confocal and conventional microscopic imaging systems have been built which share the same objective and tube lenses with a flip mirror to switch between the two imaging modes. A super-luminescent diode light with the spectrum peak at wavelength of 860 nm is used as a light source for confocal system. The output from a single mode fiber and a fiber collimator is focused onto the jet through an infinity-corrected objective lens with a numerical aperture (NA) of 0.3. The backscattered light from the sample is collected by the same objective and then focused onto a 40 μm diameter pinhole through a tube lens with a focal length of 20 cm. The pinhole is conjugate to the focus of the objective lens so that the signals that arise from the focus pass through the pinhole and signals from out-of-focus planes are largely blocked. This ensures that the information is obtained mainly from a specific point of the sample and gives the imaging system an optical sectioning property. The signal is first detected in photons by a photomultiplier tube and then electronically amplified and sent to a gate generator (Stanford SR250), which is triggered by the signal generator that applies the perturbation to the nozzle. The gate and signal output from the gate generator show the exact timing relation of the sample gate with respect to the signal which are both send to an oscilloscope (LeCroy 9304A 200MHz) for data process and analysis.

For the conventional microscopic imaging, an illuminator is used as light source with a spot size of ~5 mm diameter on the jet. A CCD camera with a minimum exposure time of 1 μs records the bright field image of the jet with single shot. By fine adjustment of the frequency of the signal generator close to a multiple of the CCD frame rate, we could obtain a pseudo-sequence of images showing the evolution of drop formation.

The equilibrium surface tension σeq of the samples was measured by a pendant drop analysis tensiometer (FTÅ 200, First Ten Ångstroms, USA). We showed the variation of σeq with surfactant concentration c in Figure 2. The cmc of SDS and Surfynol 465 is 8 mM (0.23% by wt) and 13 mM (0.9% by wt), respectively. The surface excess Γeq can be determined below the cmc from the slope of σ vs lnc according to the Gibbs equation of Γeq = –1/(nRT)·dσ/d(lnc), where n = 1 for non-ionic surfactants and n = 2 for ionic surfactants, R is the gas constant and T is the absolute temperature. SDS has a surface excess of 3.9 × 10–6 mol m–2 near its cmc which is higher than that of Surfynol 465, 2.0 × 10–6 mol m–2, reflecting the presence of two bulky hydrophobic groups in Surfynol. Surfynol 465 is, however, both more effective and more efficient than SDS as a surfactant.

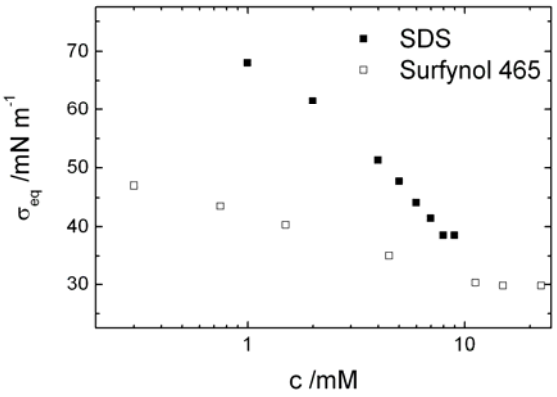

Figure 2. *Plot of σ_{eq} vs lnc for SDS and Surfynol 465 samples.*

The unperturbed liquid jet with a mean velocity of 5.6 m s^{-1} has a jet diameter of 103 μm, which is slightly larger than that the diameter of the nozzle due to wetting of the nozzle face. Figure 3 shows the response of the detector in the confocal set up when the front surface of the jet front is scanned through the focus of the laser beam. Z_o is the translation of the jet along the optical axis of the laser beam and z is the distance of the laser beam from the nozzle plate along the axis of the jet. The full-width at half-maximum of the optical axial response for the front surface is 13.1 μm. The maximum intensity corresponds to the location of the surface of the jet at the focus of the laser beam; the jet surface can be determined with an accuracy of ~ 1 μm. To achieve a higher resolution in surface profiling, the quasi-linear slope of the confocal axial response curve from Z_o = -7.8 μm to -3.7 μm can be used. Assuming the surface height variation of the sample is within this dynamic range of ~ 4.1 μm, the surface displacement ΔD is proportional to the change in the detected signal intensity d ΔI: ΔD = ΔI/S, where S is the gradient of the quasi-linear slope inside the confocal axial response curve. For our system, S = 50.5 mV/μm. The resolution is limited mainly by the mechanical stability, fluctuation of light source and electronic noise. The intensity fluctuation at a steady jet surface is <4 mV, gives a depth discrimination better than 80 nm. This enables us to study jet instability with much higher resolution than by conventional microscopy.

Figure 4 showed conventional images of the water jet with a perturbation frequency f of 11.8 kHz and wavelength λ of 480 μm. According to Rayleigh's linear stability analysis, the radial displacement δ of a cylindrical jet of incompressible inviscid liquid that is subject to infinitesimal axisymmetric oscillations of the surface grows exponentially for $2\pi a/\lambda < 1$, where a is the radius of the unperturbed jet and λ is the jet wavelength. The displacement has the form of

$$\delta(z,t) = \delta_0 e^{\alpha t} e^{ik(z-u_0 t)} \tag{2}$$

where δ0 is the initial amplitude of the disturbance, u0 is the jet velocity which, obeys u0 = λf, α is the growth rate and the wave number k = 2π/λ. Weber deduced a dispersion relation between α and k for a Newtonian fluid [4]:

$$\alpha^2 \frac{ka}{2}\frac{\mathrm{I}_0(ka)}{\mathrm{I}_1(ka)} + \alpha\nu k^2\left[2ka\frac{\mathrm{I}_0(ka)}{\mathrm{I}_1(ka)}\frac{l^2}{l^2-k^2} - 1 - 2la\frac{\mathrm{I}_0(la)}{\mathrm{I}_1(la)}\frac{k^2}{l^2-k^2}\right] = \frac{\sigma k^2 a^2}{2\rho a^3}(1-k^2a^2), \quad (3)$$

where l2 = k2+α/ν, ν = μ/ρ, ρ, μ and σ denote the fluid density, viscosity and surface tension, respectively, and I0 and I1 are hyperbolic Bessel functions of the first kind of order 0 and 1, respectively. a is the initial jet radius.

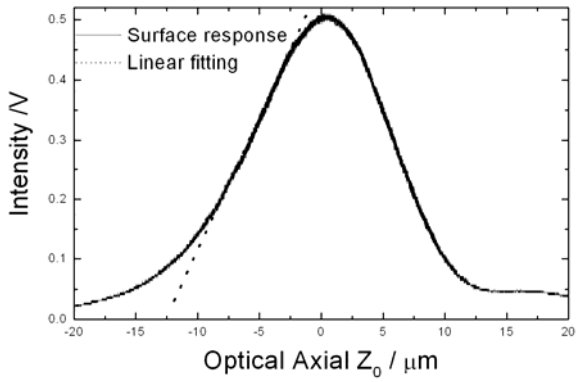

Figure 3. *Confocal response of the jet front surface (solid) and linear fitting (dotted) of the quasi-linear slope of the response; 1 mm from nozzle plate.*

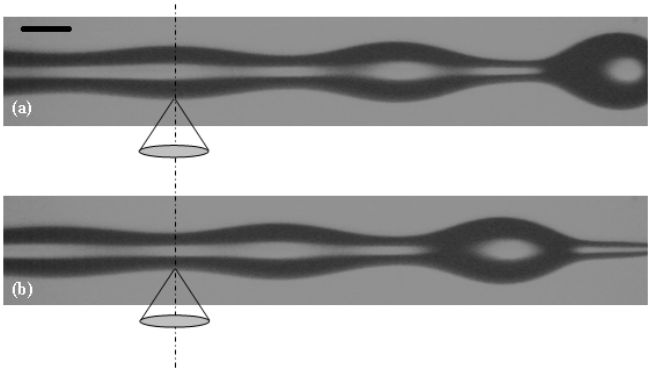

Figure 4. *(a) and (b) successive frozen images of perturbed liquid jet with an exposure time of 1 μs and an interval of 42 μs. Modulation frequency 11.8 kHz. Wavelength 480 μm. The sketched lens and beams in (a) and (b) focusing on jet swell and neck illustrate how the jet surface is located by confocal microscopy.*

By confocal imaging, we are able to locate the jet surface and measure the oscillation amplitude from a very early stage. Figure 5 plots the amplitude of oscillation determined from the difference in positions of the swell and neck against the jet axial position, z, for water, 5 mM SDS (0.14% wt), 8 mM SDS (0.23% wt), 1.5 mM Surfynol (0.1% wt) and 11.3 mM Surfynol 465 (0.75% wt). The data are plotted semi-logarithmically and linearly fitted over an axial spans of ~ 4λ ≈ 2 mm, or in term of time ~ 0.4 ms, with αz/u0, where u0 = λf = 5.664 m/s is used for f = 11.8 kHz and λ = 480 μm. Here a uniform velocity profile of the jet is assumed after z > 3 mm. In addition, for surfactant jets the DST is actually an average value over the time range of 0.4 ms. The slope gives the growth rate αwater = 7660 s-1, α5mMSDS = 7210 s-1, α8mMSDS = 6540 s-1, α1.5mMSurfynol465 = 6700 s-1, and α11.3mMSurfynol465 = 5040 s-1, for ka = 0.674. The typical error for the linear fitting is ~ 100 s-1. Hence dynamic surface tension can be deduced from the measured growth rate by equation 3. Jet diameter of 103.0 μm is fitted to get water surface tension of 72.4 mN/m which is used as a calibration value and the physical properties of water ρ = 998 kg/m3, μ = 0.955 × 10-3 Pas were used for the temperature of 22 °C for all samples. The measured dynamic surface tension of SDS and Surfynol 465 is listed in Table 1 below along with the equilibrium values.

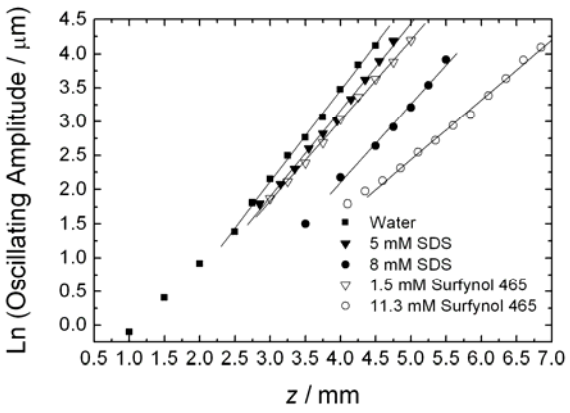

Figure 5. *Growth rate measurement of water, SDS and Surfynol 465 solution jets.*

Table 1: DST and σ_{eq} of SDS and Surfynol 465

Sample	Surface age (ms)	DST (mN/m)	σ_{eq} (mN/m)
5 mM SDS	0.7 ± 0.2	64.3 ± 2.0	47.7
8 mM SDS	0.9 ± 0.2	53.3 ± 1.8	38.5
1.5 mM Surfynol 465	0.7 ± 0.2	55.8 ± 1.8	40.5
11.3 mM Surfynol 465	1.1 ± 0.2	32.2 ± 1.4	30.6

A typical diffusion coefficient for a nonionic surfactant of the size of Surfynol 465 would be 3 × 10–10 m2 s–1. Equation 1 then gives a diffusion time of 1.5 ms for the 1.5 mM solution (using a value of Γeq= 1.4 × 10–6 mol m–2 from Fig. 2 and the Gibbs equation) and 50 μs for the 11.3 mM solution. We would therefore expect the high concentration solution to have very nearly reached equilibrium but the low concentration solution to be only partially equilibrated, which is what we observe. For SDS, τd ~0.5 and 0.2 ms at 5 mM and 8 mM, respectively, which are close enough to the surface age that a detailed mass transport model is required to establish whether or not adsorption is diffusion-controlled.

Surfactants lower the dynamic surface tension and consequently reduce the growth rate of the jet instability. As a result the jet breakup length increases. Figure 6 shows how the jet breakup length dependence on the jet velocity for the four surfactant solutions. Despite the differences in dynamic surface

tension, the final stages of ligament rupture are very similar for water and surfactant solutions.

Figure 7 shows the time delay between a swell and the following neck at fixed z, measured by confocal imaging. The insets show the temporal variation in the detected signal near the pinch-off point when the laser is focused on the neck. For the early stage of jet instability, the delay between swell and neck remains nearly constant, as would be expected for a symmetric perturbation. Downstream of z ≈ 4.2 mm in the water jet, the reflected 'pulse' becomes asymmetric. At z = 4.44 mm, the pulse broadens owing to the formation of a ligament between two swells with a sharp peak indicating a pinch at the end of the ligament near the fore swell The further development of the ligament involves the movement of the first pinching point towards the fore swell and appearance of another pinch at the other end of the ligament at z = 4.57 mm. The time scale t0 measured from final stage of perturbation growth with appearance of first pinch peak at z = 4.44 mm to eventually jet breakup at z = 4.70 mm is ~ 46 μs. This agrees very well with the time scale given by the balance of surface tension and inertia at low viscosities [5], i.e. $t0 = (\rho a3/\sigma)1/2 = 43$ μs. The temporal profile of 11.3 mM Surfynol solution jet is rather similar with the pure water one, but with larger t0 ≈ 70 μs due to its lower surface tension value.

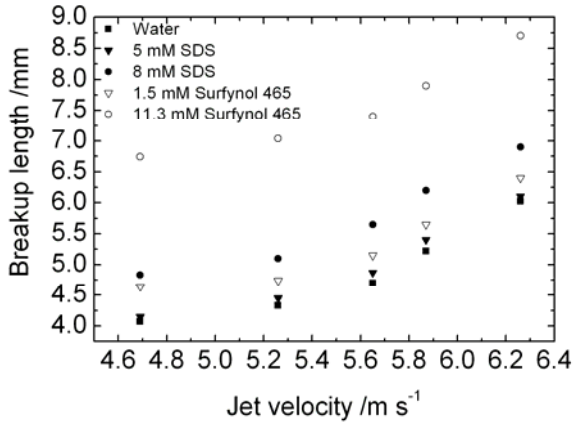

Figure 6. *Breakup length vs jet velocity for different surfactant solutions.*

The time taken for the satellite drop to be engulfed by the following drop depends on the surfactant concentration, shown in figure 8. The higher the surfactant concentration and the lower the dynamic surface tension, the longer it takes for the satellite to merge the following main drop. This result may be a consequence of momentum conservation. The momentum carried by the main drop and the satellite should equal the momentum flux of the unperturbed jet minus a surface tension contribution, integrated over one period. It has the form of [5]

$$u_0(r_m^3 u_m + r_s^3 u_s) = \frac{3\pi}{2ka}(u_0^2 a^3 - \frac{\sigma}{\rho}a^2), \qquad (4)$$

where um and us are main drop and satellite drop velocities, rm and rs are the corresponding radius respectively. In our experimental condition, um ≈ u0, where u0 >> σ/(ρau0). For the same main drop velocity, the lower the surface tension, the higher system momentum and the higher is the satellite velocity, u_s.

Acknowledgement

The authors would like to thank Philip Ash for his help with SDS recrystalization. This work is financially supported by EPSRC grant GR/T11920.

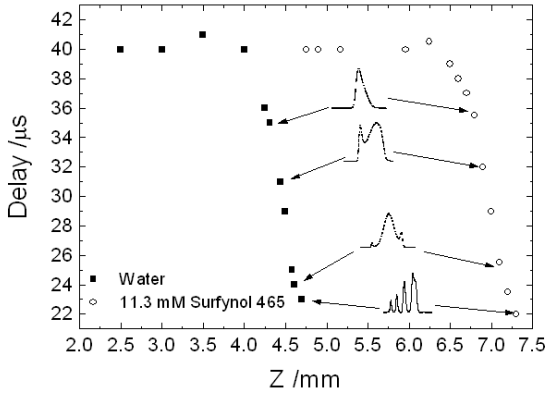

Figure 7. *The time delay along the jet axial measured between the swell and the following neck at the same axial position of the water (■) and 11.3 mM Surfynol 465 (□) jet. The corresponding ligament temporal profiles are shown.*

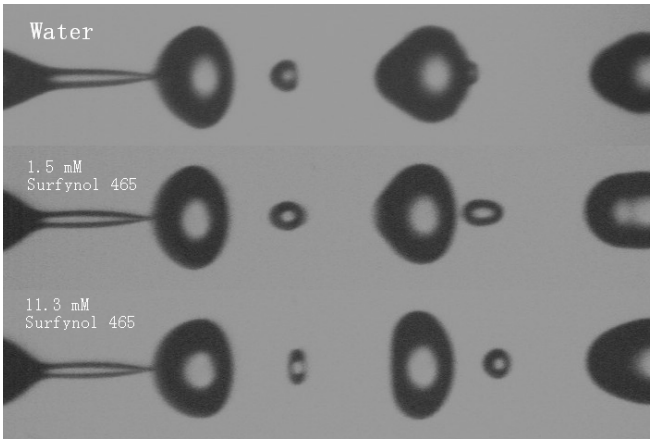

Figure 8. *The time taken for the satellite drop to be engulfed by the following drop depends on the surfactant concentration.*

References

[1] J. Eastoe, A. Rankin, R. Wat and C. D. Bain, "Surfactant adsorption dynamics," Int. Rev. Phys. Chem., 20, 357 (2001).

[2] J. D. Hines, "The preparation of surface chemically pure sodium n-dodecyl sulfate by foam fractionation," J. Colli. Interface Sci., 180, 488 (1996).

[3] L. Yang and C. D. Bain, "Study of liquid jet instability by confocal microscopy," submission to J. Fluid Mech.

[4] C. Weber, "Zum Zerfall eines Fluessigkeitssrahles." Z. Angew Math. Mech. 11, 136 (1931).

[5] J. Eggers, "Nonlinear dynamics and breakup of free-surface flows," Rev. Mod. Phys. 69, 865 (1997)

Author Biography

Lisong Yang obtained her Ph. D from Shanghai Institute of Optics and Fine Mechanics, China. She is interested in developing optical imaging technologies and finding their applications in material science. She is currently working on the project "Next Generation Inkjet Technology" in Durham University, UK.